Hindawi
International Journal of Antennas and Propagation
Volume 2022, Article ID 6886342, 8 pages
https://doi.org/10.1155/2022/6886342

Research Article

A Miniaturized Wideband Planar Bow-Tie Slot Antenna with Asymmetric CPW

Xi Chen,[1,2] **Jiasong Huang**,[1] **Chonghu Cheng**,[1] **and Leilei Liu**[1]

[1]*National and Local Joint Engineering Laboratory of RF Integration and Micro-Assembly Technology & the Institute of Flexible Electronics (Future Technology), Nanjing University of Posts and Telecommunications, Nanjing 210003, China*
[2]*Jiangsu Open University, Nanjing, China*

Correspondence should be addressed to Leilei Liu; liull@njupt.edu.cn

Received 26 November 2021; Revised 12 May 2022; Accepted 31 May 2022; Published 5 July 2022

Academic Editor: Mohammad Alibakhshikenari

In this paper, a novel miniaturized wideband planar bow-tie slot antenna is proposed. For the purpose of miniaturization and wide bandwidth, the effects of the dimension and shape of the bow-tie slot and feed structure are analyzed. This antenna adopts a water droplet slot, fed by an optimized asymmetric coplanar waveguide (CPW). By adjusting the feeding line, the impedance characteristic of the antenna is greatly improved that leads to a broader bandwidth. The proposed antenna operates from 2.8 GHz to 5.25 GHz with a gain of 3.8 dB. Compared with the traditional triangle bow-tie antenna, the relative bandwidth of the proposed antenna is broadened to more than 61%, while the size is reduced by about 36%, which indicates the proposed antenna is suitable for a variety of wireless applications.

1. Introduction

With the rapid development of wireless communication technology, higher requirements are put forward for the antenna system. Branch-line couplers are commonly used passive components in RF applications [1, 2]. Communications and medical devices require antennas with wider bandwidth and smaller sizes to be better integrated into the system. Thus, the broadband and miniaturization slot antenna is one of the hot spots.

Due to its broad bandwidth and low profile, the bow-tie antenna has been widely explored. In [3], a triangular bow-tie antenna fed by the CPW was first proposed. By adjusting the slot width and extended angle, a 36% relative bandwidth can be obtained at −10 dB [3]. To enhance the bandwidth of CPW-fed bow-tie slot antennas, some techniques have been proposed. In [3], the reconfiguration of a coplanar-fed single arm bow-tie antenna structure was proposed. It was enabled by the integration of a digital tunable capacitor (DTC) [4].

A modified bow-tie slot antenna with asymmetric slots fed by taper CPW-to-CPW transition is presented in [5]. By introducing two metal stubs in the middle of the bow-tie slot, a wider impedance bandwidth was achieved of 55% [6]. An asymmetric coplanar waveguide with different slot lengths was introduced in [7], and the impedance characteristic of the antenna is improved by adjusting the length of one asymmetric CPW slot. A pair of sector parasitic patches and a modified grounded plane can generate dual-band characteristic in Reference [8]. Another miniaturization is achieved by adding inductive strips to the capacitive 3D antenna element and thereby lowering the cutoff operational frequency to 0.85 GHz [9]. Then, the bow-tie antenna has been designed on a very thin flexible substrate with an overall impedance bandwidth of 57.7% [10]. A broadband bow-tie antenna fed by a Γ-shaped strip balun is proposed, which exhibits a good impedance bandwidth of approximately 93.3% for VSWR ≤2 ranging from 1.35 to 3.71 GHz [11]. A compound antenna composed of plane Archimedes spiral wire, sine wave spiral wire, and bow-tie antenna, which is fed by the exponential gradient microstrip balun is proposed with a wide band range of 0.95 to 3.0 GHz [12]. Based on SIW, an asymmetrical bow-tie-shaped cross slot

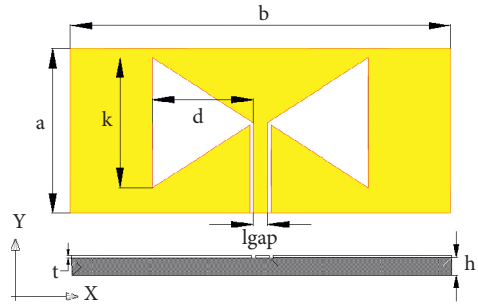

Figure 1: The geometry of antenna 1 with the conventional structure.

Table 1: Parameters of antenna 1 (mm).

a	*b*	*k*	*d*	*lgap*	*h*	*t*
25.25	53	17.5	23	2	1.6	0.0018

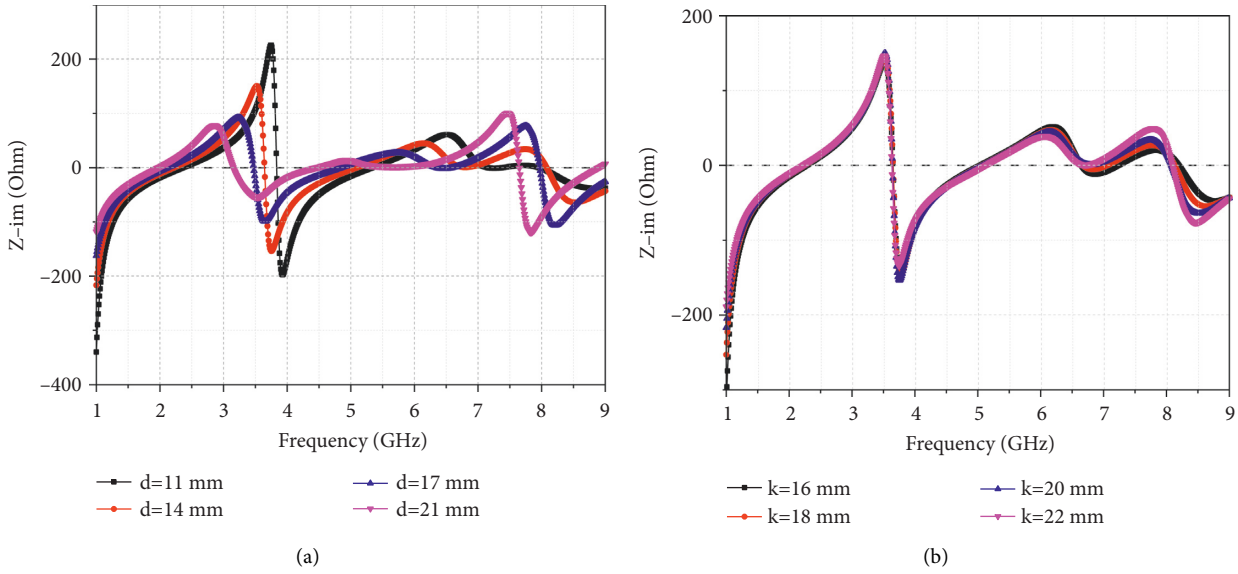

Figure 2: Imaginary parts of the input impedance of antenna 1. (a) Different d when $k = 25$ mm; (b) different k when $d = 23$ mm.

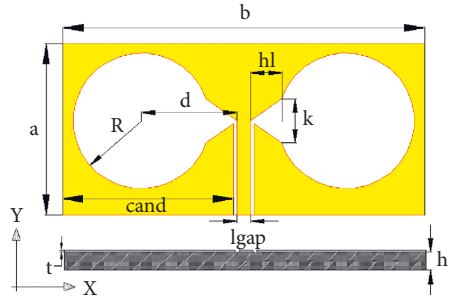

Figure 3: The geometry of antenna 2 with the water droplet slots.

radiates circularly polarized waves at two different frequencies with opposite senses of polarization [13]. And a compact dual mode wideband antenna consists of a two-element array of half-bow-tie slots operating from 24.8 to 31.6 GHz which is proposed [14]. In [15], a novel dual-polarized bow-tie antenna with a small form factor was proposed. The antenna operates over a frequency range of 3.1–5 GHz and exhibits an average gain and antenna efficiency in the vertical and horizontal polarizations of 7.5 dBi and 82.6%, respectively [15]. And a self-grounded directional bow-tie antenna offers good impedance matching across its operating frequency range with VSWR <2 and exhibits an average gain of 20 dBi for an 8×8 element antenna array [16].

Table 2: Parameters of antenna 2 (mm).

a	*b*	*k*	*d*	*hl*
25.25	53	9.04	14	4.54
cand	*R*	*lgap*	*h*	*t*
25	9	2	1.6	0.0018

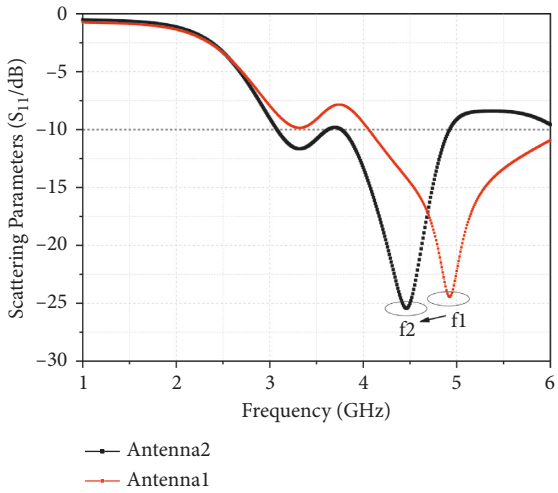

Figure 4: Reflection coefficients of antenna 1 vs. antenna 2.

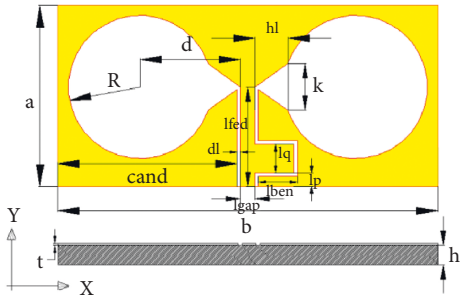

Figure 5: The geometry of antenna 3 with the ACPW.

Table 3: Parameters of antenna 3 (mm).

a	*b*	*cand*	*lgap*	*lben*	*lp*
25.25	53	25	2	5.4	1.9
lq	*lfed*	*d*	*R*	*hl*	*k*
5	13.9	14	9	4.54	9.04

In this paper, a novel miniaturized wideband planar bow-tie slot antenna is proposed. This antenna adopts two water droplet slots fed by an optimized asymmetric CPW. By bending on one side of the CPW slot, the feeding structure is formed into an asymmetric CPW. To enhance the impedance bandwidth, the slot of CPW is tapered for better impedance matching. Compared with the conventional triangular slot antennas, the proposed antenna not only has a smaller size but also has a wider operating bandwidth. The antenna design process will be presented with the analysis of simulated impedance characteristics, followed by fabrication and measurement of the antenna.

2. Antenna Design

2.1. Miniaturized Bow-Tie Slot. As shown in Figure 1, the antenna 1 is a conventional triangular bow-tie slot, which is designed on a single layer of substrate FR4 with relative permittivity $\varepsilon_r = 4.4$ and thickness $H = 1.6$ mm. The antenna

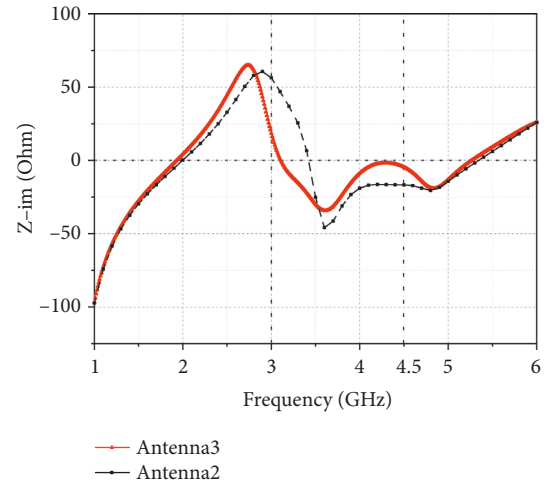

Figure 6: The imaginary parts of input impedance of antenna 2 and antenna 3.

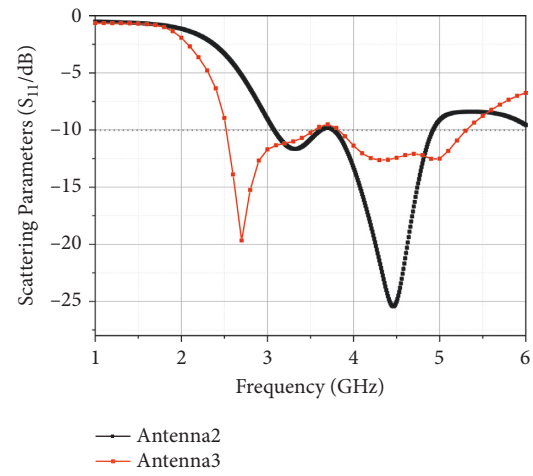

Figure 7: Reflection coefficients of antenna 2 and antenna 3.

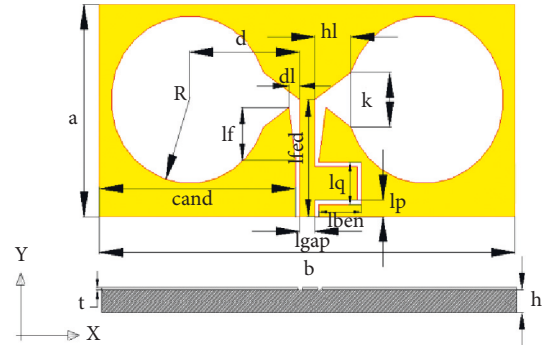

Figure 8: The geometry of antenna 4 with the taper ACPW-fed slot.

Table 4: Parameters of antenna 4 (mm).

a	*b*	*cand*	*lgap*	*lben*	*lp*	*lq*
25.25	53	25	2	5.4	1.9	5
lfed	*d*	*lf*	*dl*	*R*	*hl*	*k*
13.9	14	6.3	1.37	10	4.54	9.04

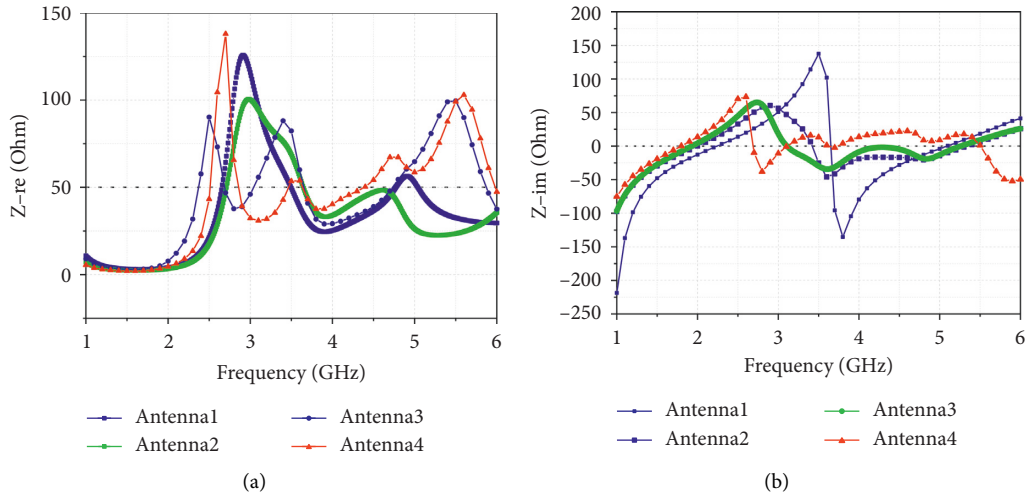

FIGURE 9: Input impedance comparison of four antennas. (a) Real parts of input impedance of antenna 1, 2, 3, and 4. (b) Imaginary parts of input impedance of antenna 1, 2, 3, and 4.

is radiated by two symmetrical triangular slots fed by a CPW. The parameters of antenna 1 are optimized, as shown in Table 1, and the key parameter affecting the radiation characteristics is the size of the triangular bow-tie slots. In order to analyze the effects of the structure size on the operating bandwidth, the parameters are studied in Figure 1.

The imaginary part of the input impedance Z_{im} is a key parameter indicating the antenna performance. This parameter of antenna 1 for different cases of k and d are simulated, as shown in Figure 2. According to the analysis of the parameters in Figures 2(a) and 2(b), it can be seen that the size of the radiation triangular bow-tie slot obviously affects the resonant frequency and working bandwidth of the antenna. For a triangular slot, the main parameter associate with the operating frequency is the length d. In terms of the imaginary part of the input impedance, as d increases, the resonant frequency of the antenna 1 moves towards a low frequency and brings a better resonance. Figure 2(b) indicates that the height of slot k has little influence on the antenna working bandwidth because the length of the current path is affected more by the length of the slots than the height of the slots.

To achieve a miniaturized design, we improve the shape of the radiating elements from triangle slots to water droplet slots, keeping the substrate size unchanged. The geometry of antenna 2 is shown in Figure 3, and its optimized size parameters are shown in Table 2. The reflection coefficients of antenna 1 and antenna 2 are compared in Figure 4. The resonant frequency of antenna 2 at $f2$ is significant lower than the antenna 1 at $f1$. It illustrates miniaturization implemented by the water droplet slots, which also brings a wider relative bandwidth. Figure 5 is shown.

2.2. Wideband Mechanism. In order to increase its working bandwidth, we improve the feed structure of antenna 2 to antenna 3 maintaining the same substrate size. Antenna 3

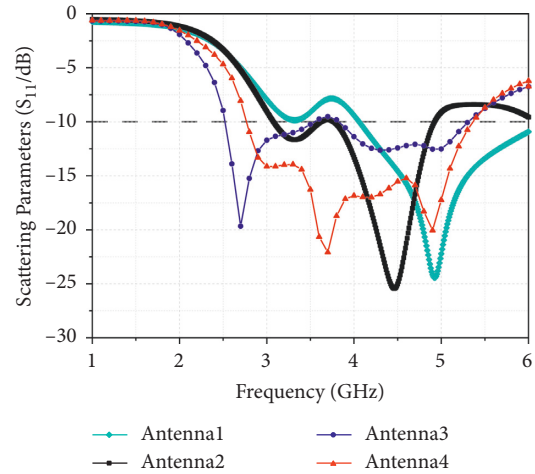

FIGURE 10: Reflection coefficient comparison of antenna 1, 2, 3, and 4.

keeps the radiation slots of antenna 2 unchanged and changes the feeding structure to an asymmetric coplanar waveguide (ACPW). A branch is added between the gap on the right side of the CPW signal and the ground, which makes the gap length of the feeding gap on the right side larger than that on the left side. The length of the branch, *lben*, is about one-eighth of the wavelength of the second resonant mode of the slot antenna. In this way, the second resonant mode moves down close to the first resonant mode, so that the working frequency bandwidth expands. The geometrical parameters of antenna 3 are shown in Table 3.

To analyse the ACPW, the input impedances of antenna 2 and antenna 3 are simulated with HFSS and shown in Figure 6. By optimizing the parameter length *lben*, height *lq*, and distance *lp* of the asymmetric branch, 4 resonance points are obtained in the working band of antenna 3. Compared with antenna 2, an additional resonance point is added within 4 GHz to 4.5 GHz by the asymmetric branch, which also makes all resonant frequencies move lower. Figure 7 shows the simulated reflection coefficient results of antenna

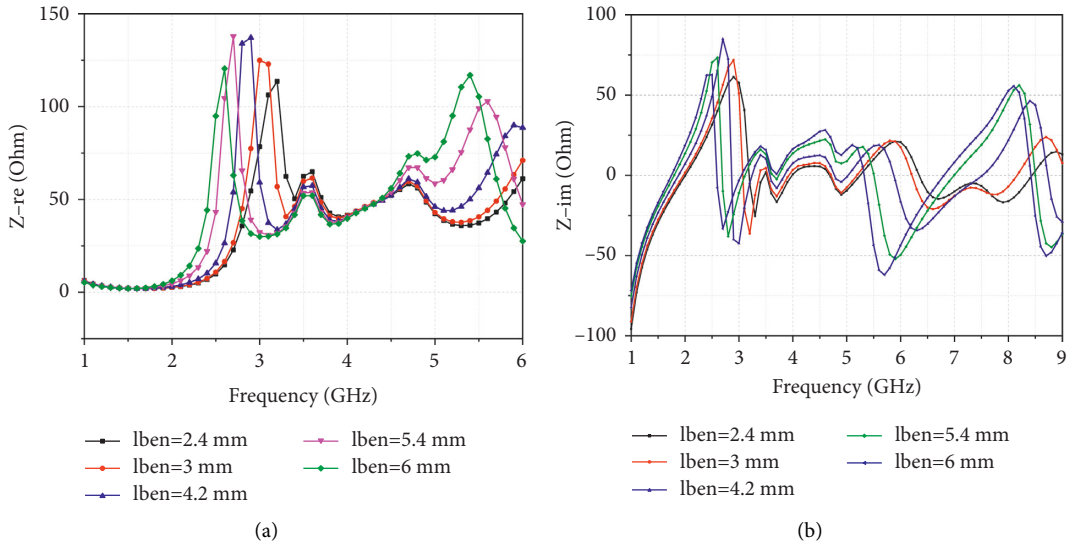

Figure 11: Input impedance of antenna 4 with a different parameter *lben*. (a) The real part of input impedance. (b) The imaginary part of input impedance.

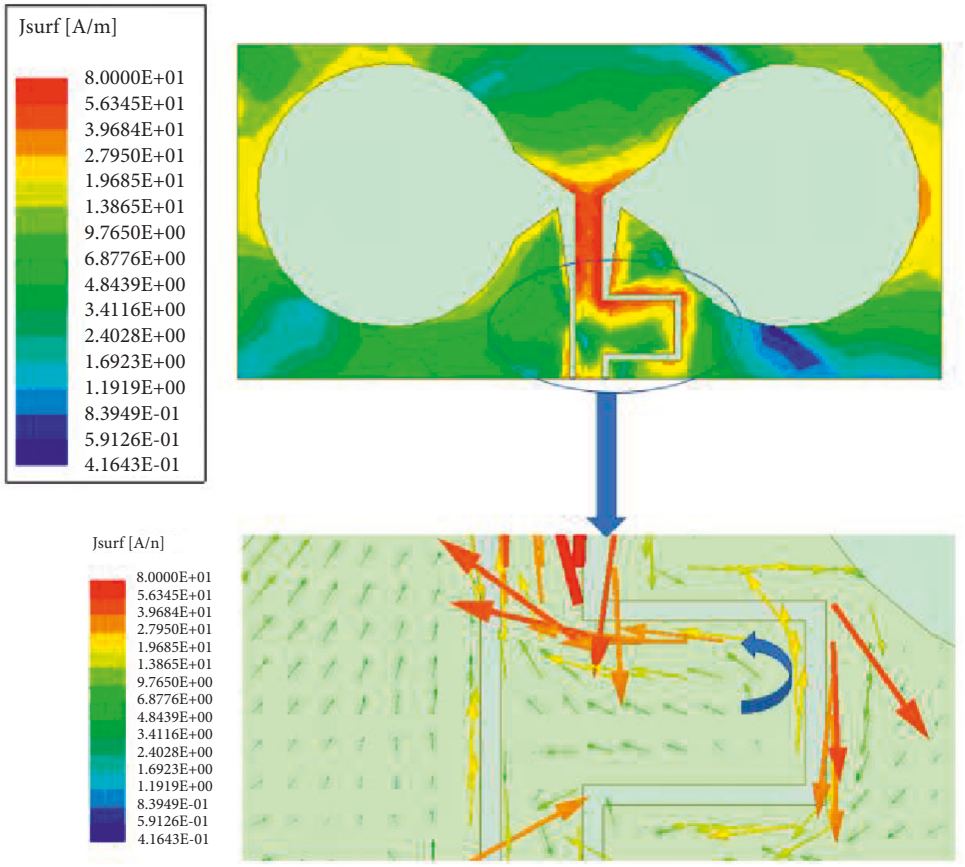

Figure 12: The surface current distribution of antenna 4 at 4.5 GHz.

2 and antenna 3. It can be clearly seen from the S11 parameters that compared with antenna 2, the bandwidth of antenna 3 increases significantly.

In general, the characteristic impedance of slot antennas is bigger than the CPW-fed impedance of 50Ω. Thus, the existence of impedance mismatch results in bandwidth

limitation of slot antennas. In the structure of antenna 4, the feeding slots are tapered by triangular angles around the ground conductor of CPW near radiation slots, as shown in Figure 8. The geometry parameters of antenna 4 are shown in Table 4.

In this work, the wideband mechanism is studied with the input impedance of four antenna structures shown in Figure 9. A zero imaginary part of input impedance corresponding to a resonant frequency and 50Ω real part of input impedance achieves the impedance match. At the resonant frequencies, the real part of input impedance of antenna 4 is closer to 50 Ω, indicating a good reflection performance since all the antennas are fed by 50 Ω. Even though the antenna 3 shows better performance below 3 GHz, five resonant frequencies and the best performance on the whole working band can be observed in antenna 4 benefited from the taper ACPW-fed slot. It indicates a good reflection coefficient and a wide bandwidth. The reflection coefficients of these four antennas are shown in Figure 10 corresponding to the above analysis.

After analyzing the reflection coefficients of antenna 4, it is found that *lben* is a major parameter influencing the reflection coefficients. Figure 11 shows the input impedance of antenna 4 with a different parameter *lben*. Obviously, when lben is 5.4 mm, the imaginary part of impedance has the largest number of resonance points within the working band, while the real part is closest to 50 Ω.

2.3. Surface Current Distribution. It is considered that the radiation of the slot antenna can be generated by the magnetic current in the radiation slot. However, if the conductor plane of the slot antenna is finite, it is not sufficient to analyze only the magnetic current in the radiation slot. In this case, it is more convenient to analyze the radiation by the surface electric current. Figure 12 shows the surface current distribution on the surface of the antenna 4 conductor simulated at 4.5 GHz. It can be found that the surface current mainly concentrates on both left and right edges of the radiation slot with the same direction, which produces copolarization radiation of the slot antenna.

The inner illustration shows the surface current distribution of the asymmetric coplanar waveguide. Due to the increasing length of the slot path on the right side of ACPW, the cascaded capacitance increases and causes the resonant frequency of the antenna to decrease [4]. Meanwhile, the additional slot path may extend the current path, which means some higher-order mode resonant frequencies of the radiation slot may decrease.

3. Results and Discussion

In this section, the simulated and measured performances of antenna 4 with the parameters of Table 4 are presented, and the fabricated structure is shown as Figure 13. According to the simulated and measured reflection coefficients as shown in Figure 14, the measured bandwidth under −10 dB of the proposed antenna is 2.45 GHz (2.8 GHz–5.25 GHz) with the FBW of 61%. Figures 15 and 16 are the patterns of E plane and H plane at 3.5 GHz, respectively. Obviously, the gain of cross-polarization is far less than the gain of copolarization on both E plane and H plane, which indicates well performance in the radiation sector of the proposed antenna. Due to the measurement error, the measured gain of

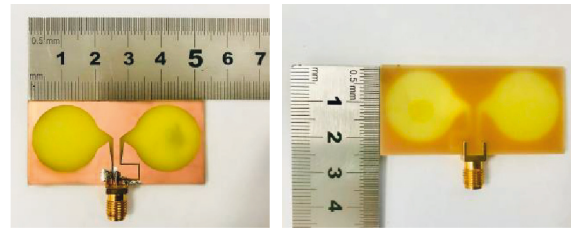

Figure 13: Fabricated structure of the proposed antenna.

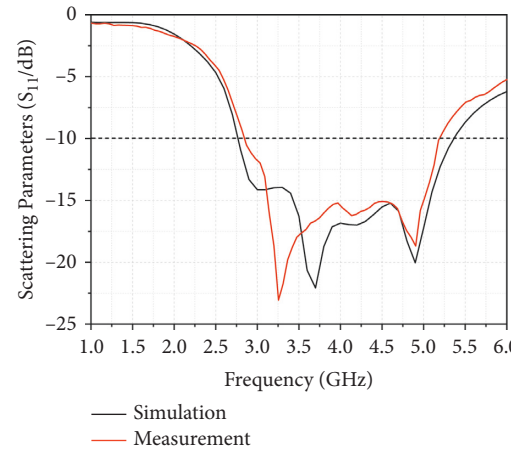

Figure 14: Reflection coefficient of the proposed antenna.

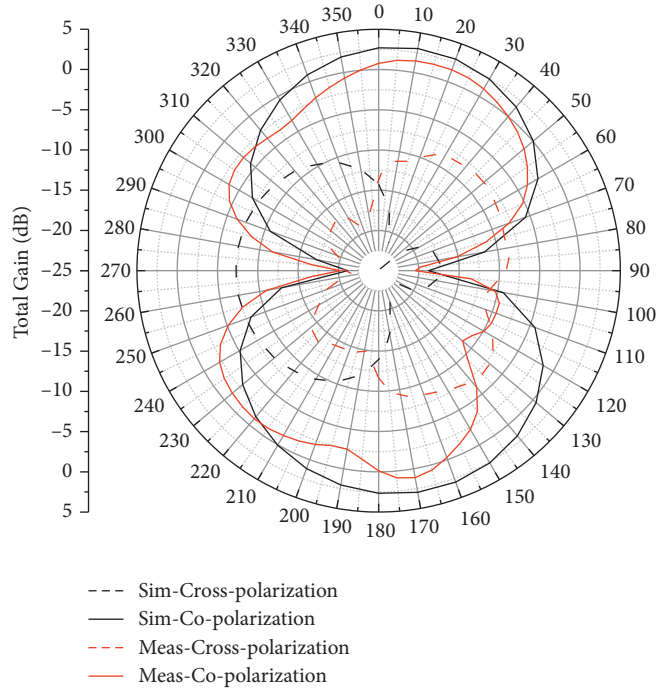

Figure 15: Radiation E plane of the proposed antenna.

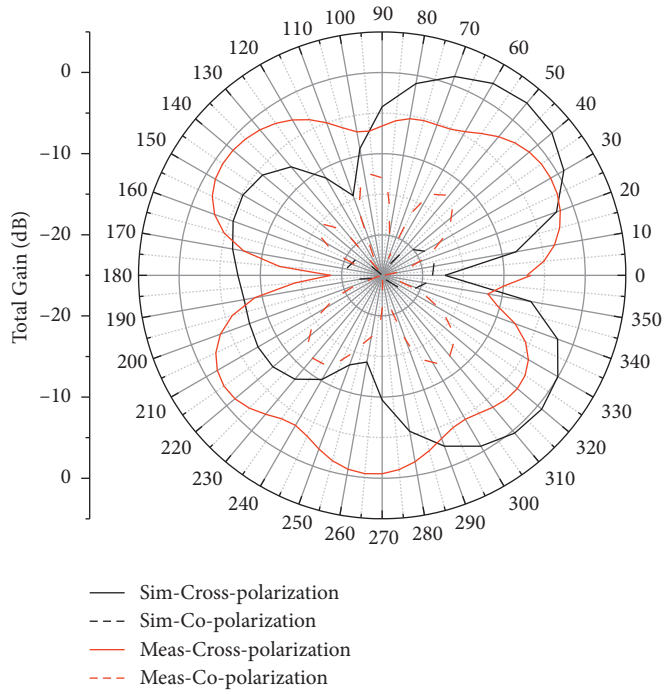

Figure 16: Radiation H plane of the proposed antenna.

Table 5: Performance comparison of bow-tie antennas.

Reference	Size (mm^2)	Bandwidth (GHz)	Radiation gain (dB)	FBW (%)	Electrical dimension
[4]	$50 \times 50 \times 10$	1.9–2.3	3.17	20	$0.14\lambda \times 0.14\lambda$
[6]	84.92×63	1.75–2.6	3	55	$0.50\lambda \times 0.37\lambda$
[8]	34×68	4.2–5.15	—	32.8	$0.48\,\lambda \times 0.95\lambda$
[10]	60×80	2.21–4	6.2	57.7	$0.44\lambda \times 0.59\lambda$
[15]	$32 \times 32 \times 33.8$	3.1–5	7.5	42	$0.4\lambda \times 0.4\lambda$ (footprint)
Proposed antenna	25.25×53	2.8–5.25	3.8	61	$0.24\lambda \times 0.49\lambda$

copolarization on E plane is 3.8 dB, which is only less than the simulated result with 1.15 dB. Measured results of reflection coefficients and patterns agree well with simulations.

A brief comparison between various bow-antennas is presented in Table 5 to highlight their sizes and bandwidths. It is necessary to note that the electrical dimension corresponds to the free space wavelength of the lowest operating frequency, which indicates an objective evaluation of antenna miniaturization. According to Table 5, the proposed antenna has a smaller electrical dimension with wider fractional bandwidth.

4. Conclusions

In this paper, a miniaturized wideband planar bow-tie slot antenna with the improving feeding structure and radiation slot is proposed. The influences of the size and shape of the radiation slot on the working frequency and bandwidth of the planar bow-tie slot antenna have been analyzed. The water drop-shaped radiation slot and asymmetric CPW feeding structure broaden the bandwidth and realize the miniaturization of the antenna effectively. The impedance characteristics of the antenna can be further tuned by a gradual transition structure between the asymmetric CPW and the radiation slot. Compared with the reference, the proposed antenna has smaller electrical dimension and wider fractional bandwidth. The proposed antenna operates from 2.8 GHz to 5.25 GHz with a fractional bandwidth of 61% and gain of 3.8 dB.

Data Availability

Data are included within the manuscript.

Conflicts of Interest

The authors declare that they have no conflicts of interest.

Acknowledgments

This work was supported by the Natural Science Foundation of China under Grant no. 62001250.

References

[1] A. Pirasteh, S. Roshani, and S. Roshani, "Compact microstrip low pass filter with ultrasharp response using a square-loaded modified T-shaped resonator," *Turkish Journal of Electrical*

Engineering and Computer Sciences, vol. 26, no. 4, pp. 1736–1746, 2018.

[2] H. Siahkamari, M. Jahanbakhshi, H. N. Al-Anbagi, A. A. Abdulhameed, M. Pokorny, and R. Linhart, "Trapezoid-shaped resonators to design compact branch line coupler with harmonic suppression," *AEU-International Journal of Electronics and Communications*, vol. 144, Article ID 154032, 2022.

[3] J. F. Huang and C. W. Kuo, "CPW-fed bow-tie slot antenna," *Microwave and Optical Technology Letters*, vol. 19, no. 5, pp. 358–360, 1998.

[4] F. A. Asadallah, A. Eid, G. Shehadeh, J. Costantine, Y. Tawk, and E. M. Tentzeris, "Digital reconfiguration of a single arm 3-D bowtie antenna," *IEEE Transactions onAntennas and Propagation*, vol. 69, no. 7, pp. 4184–4188, 2021.

[5] C. Y. Huang and D. Y. Lin, "CPW-fed bow-tie slot antenna for ultra-wideband communications," *Electronics Letters*, vol. 42, no. 19, p. 1073, 2006.

[6] L. Marantis and P. Brennan, "A CPW-fed bow-tie slot antenna with tuning stub," in *Proceedings of the LAPC*, pp. 389–392, IEEE, Loughborough, UK, March 2008.

[7] L. Xu, L. Li, and W. Zhang, "Study and design of broadband bow-tie slot antenna fed with asymmetric CPW," *IEEE Transactions on Antennas and Propagation*, vol. 63, no. 2, pp. 760–765, 2015.

[8] H. W. Liu, X. Zhan, S. Li, J. H. Lei, and F. Qin, "Dual-band bow-tie slot antenna fed by coplanar waveguide," *Electronics Letters*, vol. 50, no. 19, pp. 1338–1340, 2014.

[9] M. Jalilvand, X. Li, J. Kowalewski, and T. Zwick, "Broadband miniaturised bow-tie antenna for 3D microwave tomography," *Electronics Letters*, vol. 50, no. 4, pp. 244–246, 2014.

[10] M. O. Sallam, S. M. Kandil, V. Volski, G. A. E. Vandenbosch, and E. A. Soliman, "Wideband CPW-fed flexible bow-tie slot antenna for WLAN/WiMax systems," *IEEE Transactions on Antennas and Propagation*, vol. 65, no. 8, pp. 4274–4277, 2017.

[11] Y. Q. Zhang, S. T. Qin, and L. X. Guo, "Novel broadband bow-tie antenna with high-gain performance using electromagnetic coupling feed," *International Journal of RF and Microwave Computer-Aided Engineering*, vol. 29, no. 1, Article ID e21478, 2019.

[12] Y. Wang, C. Feng, J. Guan, and J. Liu, "A multi frequency point broadband compound antenna for partial discharge detection in gas insulated switchgear," *International Journal of RF and Microwave Computer-Aided Engineering*, vol. 30, no. 12, Article ID e22433,, 2020.

[13] K. K. S Priya, S. Dwari, and S. Dwari, "Substrate integrated waveguide dual-frequency dual-sense circularly polarized cavity-backed slot antenna," *International Journal of RF and Microwave Computer-Aided Engineering*, vol. 29, no. 12, Article ID e21987, 2019.

[14] M. Ali, K. K. Sharma, R. P. Yadav et al., "Design of dual mode wideband SIW slot antenna for 5G applications," *International Journal of RF and Microwave Computer-Aided Engineering*, vol. 30, no. 12, Article ID e22449, 2020.

[15] M. Alibakhshikenari, B. S. Virdee, C. H. See et al., "Dual-polarized highly folded bowtie antenna with slotted self-grounded structure for sub-6 GHz 5G applications," *IEEE Transactions on Antennas and Propagation*, vol. 70, no. 4, pp. 3028–3033, 2022.

[16] M. Alibakhshikenari, S. M. Moghaddam, A. U. Zaman, J. Yang, B. S. Virdee, and E. Limiti, "Wideband sub-6 GHz self-grounded bow-tie antenna with new feeding mechanism for 5G communication systems," in *Proceedings of the 13th European Conference on Antennas and Propagation (EuCAP 2019)*, pp. 1–4, Krakow, Poland, April 2019.